Journal of Ovonic Research Vol. 13, No. 3, May - June 2017, p. 113 - 118

# FEATURES OF THERMAL AND ELECTRICAL PROPERTIES OF GaSb-CrSb EUTECTIC COMPOSITE

R. N. RAHIMOV[a], M. V. KAZIMOV[a *], D. H. ARASLY[a], A. A. KHALILOVA[a], I. K. MAMMADOV[b]
[a]*Institute of Physics of the National Academy of Sciences of Azerbaijan, Baku Az - 1143, Baku, H. Javid ave.33;*
[b]*Azerbaijan National Academy of Aviation, Baku, Az-1057 Republic of Azerbaijan, Baku. Mardakan ave. 30*

In GaSb-CrSb eutectic composite, the electrical and thermal conductivity, thermoelectric power and Hall coefficients were investigated in a wide temperature range. The thermal conductivity has been analysed in the framework of Callaway model. The observed anisotropy of thermal conductivity explained with long–wave phonon scattering at boundaries between the semiconductor and metal phases when thermal flow is perpendicular to metallic inclusions. The addition thermal conductivity, observed above 200K is associated with the resonance energy transfer and was approximated by Koshino and Ando theory.

(Received January 24, 2017; Accepted May 22, 2017)

*Keywords:* Eutectic composite, XRD,SEM and EDX analysis, Thermal and electrical conductivity, Thermoelectrical power, Hall coefficient

## 1. Introduction

Microelectronics development depends on novel with controlled properties materials. For this purpose the eutectic composites based on III-V compounds and 3d-metals, where the metallic phase with needle-shaped are form and oriented parallel in the matrix, may be used for galvanomagnetic, thermomagnetic, photothermomagnetic and strain sensitive translators [1-3]. The advantage of such compositions is the combination of semiconductor and metal properties. GaSb-CrSb eutectic composite, as one of heterogeneous semiconductors, consists from diamond-like GaSb and compound CrSb with hexagonal structure. The NiAs type CrSb compound is antiferromagnetic below about 700K, where the magnetic moments of Cr ions are directed along the c-axis, aligned ferromanetically in the c-plane, and antiferromagnetically in the adjacend c-planes [4]. From this point of view GaSb-CrSb eutectic composite, as deluted magnetic semiconductor may be one of the promising material for spintronic devices [5, 6].

Previously, by XRD analysis it was confirmed that GaSb-CrSb composite has a two-phase structure [7, 8]. Heat flow and heat capacity studies have been made in the 293-1273K temperature range, and enthalpy of fusion and specific heat were determined. The initial and final points of melting temperature are determined as 943K and 965K, respectively [8].

The present work is focused on the electron micrographic analyses, electrical and thermal conductivity of GaSb-CrSb composite.

## 2. Experimental

GaSb-CrSb eutectic composites were prepared by using the vertical Bridgman method. The rate of the crystallization front was about (0.3÷0.6) mm/min. XRD intensity data were collected on an Advance-D8 diffractometer using CuKα radiation. A Zeiss ΣIGMA Field Emission

*Corresponding author: mobilkazimov@gmail.com

Scanning Electron Microscope (FESEM), equipped “Oxford EDS” и “HKL EBSD”, were used to characterize the morphology of the specimens and to obtain qualitative information on the elemental composition of the samples, respectively. Samples for electric measurement were prepared in a parallelepiped form with size (2×4×10)$cm^3$. On the both lateral sides of the samples, four contact probes were attached to measure the electrical conductivity (σ), thermal power (α) and Hall coefficient (R) using the compensation method, and the thermal conductivity (K) was measured by the absolute stationary heat flow method.

## 3. Results and discussion

Diffraction patterns of GaSb-CrSb eutectic composite are shown in Fig. 1. These figures also show data on the diffraction patterns for GaSb and CrSb compounds. Analysis of XRD spectra confirmed that this system is diphasic: the most intense peaks corresponding to the (111), (200), (220), (311), (222), (400), (331), (420), and (422) Muller index are identical to the GaSb matrix, while the weak peaks found at 2θ = 30º, 44.08º, 52.12º, and 54.13º coincide with the CrSb lines having a hexogonal structure with lattice parameters of a = 4.121, c = 5.467, c/a = 1.327, and the P63/mmc space group.

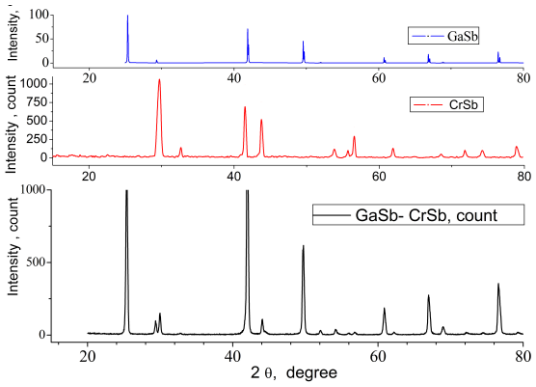


*Fig. 1. Comparative diffraction patterns of GaSb and CrSb compounds and GaSb-CrSb eutectic composite*

Based on SEM examinations (Figs.2), the needle-shaped metallic inclusions with a diameter of about 0.9-1.6 μm, a length of 20÷50 μm and a density of ~6x$10^4$ $mm^{-2}$ are uniformly and parallel distributed in the GaSb matrix. It was found that the matrix contains Ga = 36.1wt%, Sb = 63.9 wt% (Fig.3, spectrum 1), the inclusion are contained Cr = 27.8 wt%, Sb = 72.2 wt% (Fig.3, spectrum2). The data correspond to the stoichiometric composition of the matrix and inclusions. Fig.4 shows elemental maps of Cr, Ga and Sb from the cross sections along the lateral direction of the needle phases, respectively. In the specific map, the colours red, blue and green indicate Sb (L), Cr (K) and Ga (K), respectively and black colour indicates the absence of this element.

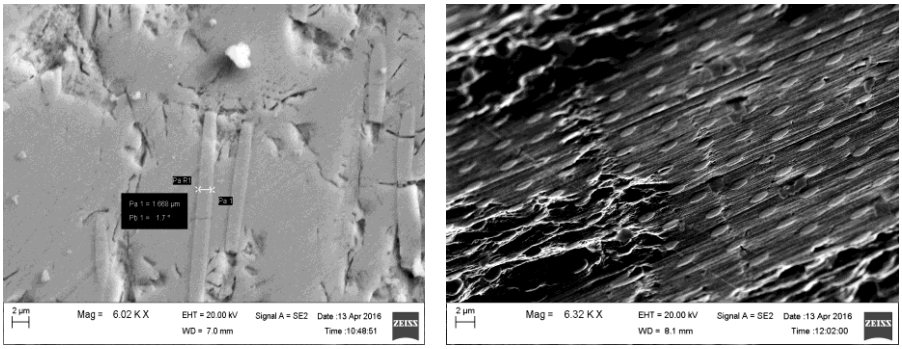


a) b)

*Fig. 2. SEM micrographs of GaSb-CrSb showing cross sections of the samples along the (a) longitudinal and (b) lateral directions of the CrSb phase*

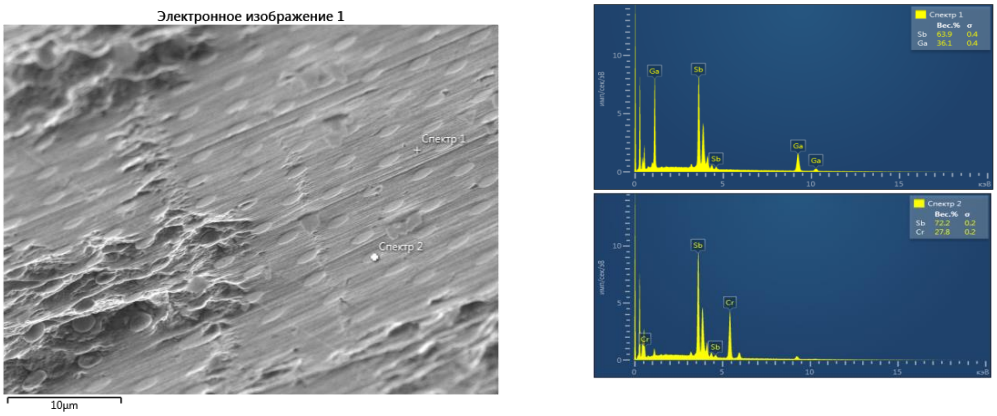


*Fig.3. X-ray spectra of GaSb–CrSb obtained with SEM–EDX from the needle and matrix phases along the lateral directions of the specimens*

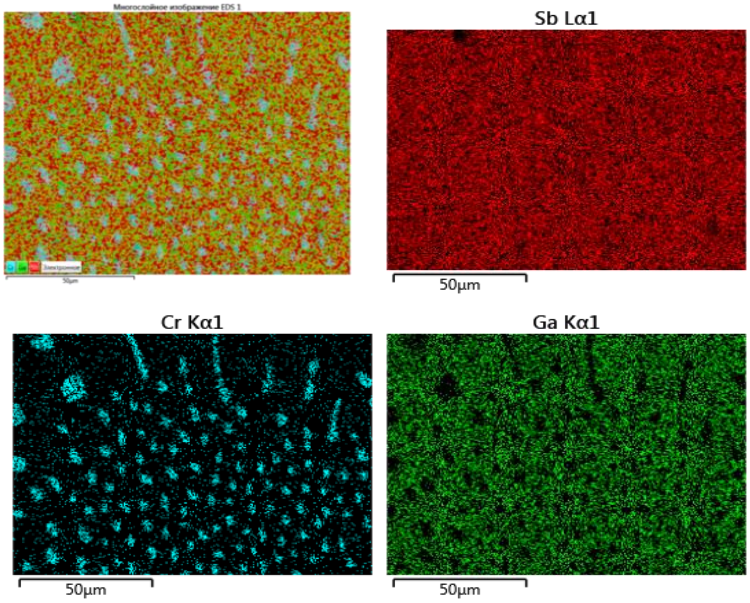


*Fig.4. Element map of the GaSb–CrSb composite*

The temperature dependence of the Hall coefficient R(T) and electrical conductivity σ(T) at the different mutual directions of current (I), magnetic field (B), and crystallization direction (x) have been measured. The Hall coefficient drops along the sample in the case of I||x⊥B due to the short-circuiting by inclusions of the current through the sample and the Hall voltage one in the case of I⊥x⊥B has a minimum value [9], because, the Hall coefficient have beenmeasured in the case of I⊥x||B, where there is no shorting of any current or Hall potential. It is evident from Fig. 5 that the Hall coefficient remains unchanged in a temperature range of 80÷475 K. The sign of the Hall coefficient changes at temperatures between 490 and 515 K (the inversion charge for GaSb is take place at 560 K).

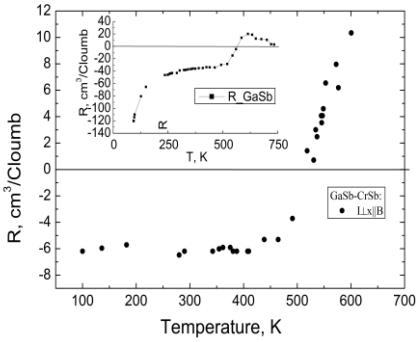


*Fig.5.Temperature dependence of Hall coefficient for GaSb-CrSb composite. (R(T) dependence for GaSb is shown in the insertion)*

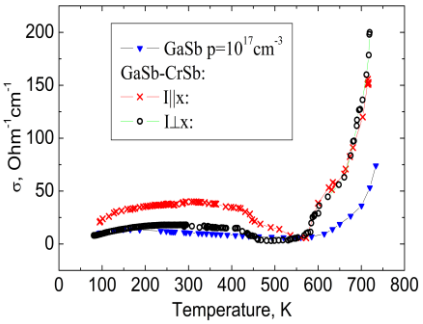


*Fig.6. Temperature dependence of electric conductivity for GaSb and GaSb-CrSb composite*

As seen from Fig.6, due to short-circuiting action by needle-shaped inclusions, the electrical conductivity in the I||x direction is significantly larger than that in the I⊥x direction. The coefficient of conductivity anisotropy at 80 K is $\sigma_{\parallel}/\sigma_{\perp}$=3.2 and decreases with increasing temperature: $\sigma_{\parallel}/\sigma_{\perp}$=3 at 300K. In the 400÷560K temperature range the σ(T) decreases in both directions, however, above 560K, greatly increases and anisotropy completely disappears. The decrease of electrical conductivity is associated with the occurrence of a new flow of conduction electrons compensating of the hole conductivity. Above 560K, the electron contribution to the conductivity and total mobility were increased. The deviation on the σ(T) dependence observed in the 600÷700K temperature range is possibly due to the magnetic phase transition of the CrSb inclusions [4,5].

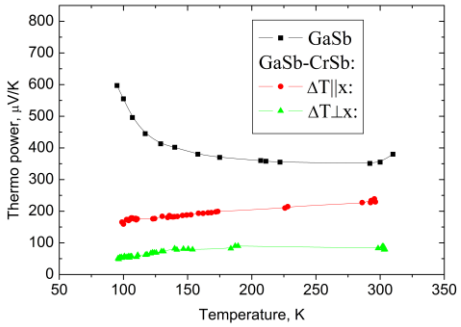


*Fig.7. Temperature dependence of thermoelectric power for GaSb-CrSb composite*

Strong anisotropy is also observed in the temperature dependence of the thermoelectric power (Fig. 7). The short-circuiting of $V_{\alpha}$ potential by metallic inclusions in ΔT||x direction is caused by a decrease in the thermopower with anisotropy degree of $\alpha_{\perp}/\alpha_{II}$=2.4.

The temperature dependence of thermal conductivity K(T) of GaSb-CrSb eutectic composite are presented on the fig. 8. Thermal conductivity up to 200K depends on temperature as $\sim T^{-0.8}$ (Fig.3). Two features are observed in the temperature dependence: the anisotropy in K(T) in parallel and perpendicular directions of metallic inclusions to the solidification front and additional thermal conductivity. At 80 K, anisotropy degree is 1.27, with temperature increasing it reduces and at room temperature disappears. The calculations have shown that free path length of the long-wavelength phonons is the same order as the transverse dimensions of metallic inclusions, which indicates the relationship of the observed anisotropy to the long-wavelength phonons scattering at the boundary inclusions.

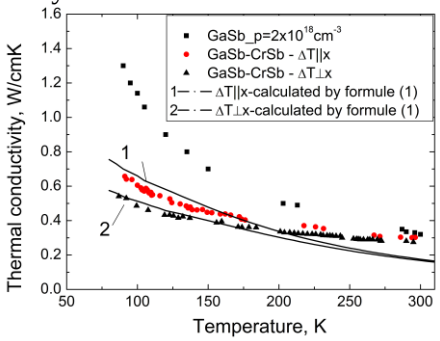


*Fig.8. Thermal conductivity of GaSb and GaSb-CrSb composite, curves 1 and 2 are calculated from the formula (1)*

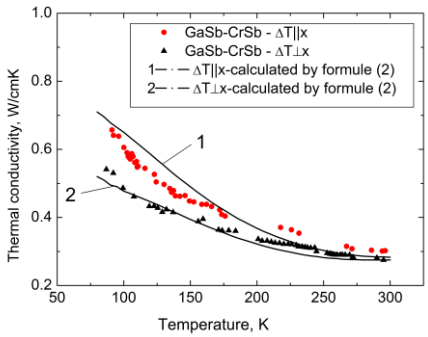


*Fig.9. Thermal conductivity of GaSb and GaSb-CrSb composite, curves 1 and 2 are calculated from the formula (2)*

The heat transfer mechanisms have been investigated in the framework of Callaway model. The total thermal conductivity of the composite is calculated taking into account contributions of the electron and phonon parts. Electronic thermal conductivity is calculated by the formula Wiedemann-Franz, and phonon thermal conductivity is for relaxation model of Callaway [10]:

$$K_f = \frac{k}{2\pi^2 v}\left(\frac{k}{\hbar}\right)^3 T^3 \int_0^{\theta/T} \frac{\tau_c z^4 e^z}{(e^z-1)^2} dz \; ; \; K_1=K_{el}+K_f, \qquad (1)$$

here θ is the Debye temperature, $z = \frac{\hbar\omega}{k_0 T}$, ω is the phonon frequency, $\tau_c$is the generalized relaxation time.

As can be seen from Fig.8, above 200K the calculated curve is below the experimental one due to the additional thermal conductivity which is 30% of the total at 300K. Most likely, in this region there are the other mechanisms of heat transfer. Such mechanisms can be magnon and photon thermal conductivity. However, calculations show that in this region, their parts in thermal conductivity are negligible. According to Koshino and Ando model [11] the resonance energy transfer can be the dominant mechanismin thermal conductivity increasing. It is known that 3d-transition metal impurities may produce the deep and shallow impurity levels in the III-V group compounds [12]. When the excited electron from a deep local level in the band gap moves into the conduction band, other conduction electron returns to the shallow level. At thermal gradient, ionization energy is transferred to the cold edge of the sample. As seen from fig.5 electrical conductivity of GaSb-CrSb eutectic composite in the range of 80÷400K prevails over the extrinsic conductivity and in this region the resonance energy transfer is expressed as follows [11]:

$$K_R = 9.5 * 10^{-2}\left(\frac{m_0}{m^*}\right)\varepsilon_\infty^{1/2} n_d^{5/4} T^{5/8}(E_d^2 + 4E_d k_B T + 6k_B^2 T^2) e^{-E_d/k_B T}$$
$$K_2=K_{el}+K_f+K_R \qquad (2)$$

Here $\varepsilon_\infty$ is the dielectric constant, $k_B$ is the Boltzmann constant, $n_d$ is the local level concentration, $E_d$ is the energy of the local level, $m_0$ is the mass of the electron. We have assumed $\varepsilon_\infty$=16 and

$E_d$=0.02eV. The total thermal conductivity calculatied by formula (2) well agrees with the experimental data (Fig. 9).

## 4. Conclusions

GaSb–CrSb eutectic alloys were prepared by the vertical Bridgman method. The two-phaseness of the GaSb-CrSb eutectic composite have been confirmed by the microstructure and morphology studies. The observed additional thermal conductivity in GaSb-CrSb is associated with the resonance energy transfer, while the anisotropy is associated with long-wavelength phonon scattering at the boundary inclusions.

## References

[1] H. Weiss, Structure and application of Galvanomagnetic devices, Pergamon Press, (1969).
[2] M.ASopovskaya, Y.S. Smetannikova, FTP (Semiconductors) **21**(7), 1242 (1987).
[3] R.N.Rahimov, A.A.Khalilova, D.H.Arasly, M.I.Aliyev, M.Tanoglu, L. Ozyuzer, Sensors and Actuators A: Physical V **147**, 436 (2008).
[4] S. Abe, T. Kaneko, M.Yoshida, K.Kamigaki, Journal of the Physical Society of Japan. **53**, 2703 (1984).
[5] S.Polesya, G.Kuhn, S. Mankovsky, H.Ebert, M.Regus, W.Bensch, J. Phys. Condens Matter. 24 (2012) 036004 (5pp).
[6] M. Shirai, J. Appl. Phys. **93**, 6844 (2003).
[7] R.N.Rahimov, I.Kh.Mammadov, M.V.Kazımov, D.H.Arasly, A.A.Xəlilova, Journal of Qafqaz University-Physics.**1**, 166 (2013).
[8] R.N.Rahimov, I.Kh. Mammadov, M.V.Kazimov, D.H.Arasly, A.A.Khalilova, Moldavian Journal of the Physical Sciences**14**, 44 (2015).
[9] M.I.Aliyev, A.A.Khalilova, D.H.Arasly, R.N.Rahimov, M.Tanoglu, L.Ozyuzer, J.Phys.D: Appl. Phys. **36**, 2627 (2003).
[10] J.Callaway, H. Baeyer, Phys. Rev. **120**, 1149 (1960).
[11] S.Koshino, T.Ando. J. Physical Society of Japan, **16**, 1151 (1961).
[12] E.M. Omelyanovskiy, V.I. Fistul, Impurity of Transition Metal in Semiconductors (in Russian) Moskow, Metallurgiya, 192 (1983).